

Robust Few-Shot Vision-Language Model Adaptation

Hanxin Wang¹, Tian Liu², Shu Kong^{1,3,*}

¹University of Macau, ²Texas A&M University, ³Institute of Collaborative Innovation
project website: <https://hannawang09.github.io/projects/srapf/>

Abstract

Pretrained Vision-Language Models (VLMs) achieve strong performance on downstream tasks when adapted with just a few labeled examples. However, the few-shot adapted models inevitably encounter out-of-distribution (OOD) test data that deviates from the in-distribution (ID) task-specific training data. Enhancing OOD generalization in few-shot adaptation is thus critically important, motivating our work on *robust few-shot VLM adaptation* for both ID and OOD accuracy. Through comprehensive comparisons of adaptation methods (e.g., prompt tuning, linear probing, contrastive finetuning, and full finetuning), we uncover three key findings: (1) finetuning with proper hyperparameters significantly outperforms prompt tuning and linear probing, which are common *de facto* methods in VLM adaptation; (2) visual encoder-only finetuning achieves better efficiency and accuracy (both ID and OOD) than contrastively finetuning both visual and textual encoders; (3) finetuning the top layers of the visual encoder provides the best balance between ID and OOD accuracy. Building on these findings, we propose partial finetuning of the visual encoder empowered with two simple augmentation techniques: (1) retrieval augmentation which retrieves task-relevant data from the VLM’s pretraining dataset to enhance adaptation, and (2) adversarial perturbation which promotes robustness during finetuning. We find that the former/latter boosts OOD/ID accuracy while slightly sacrificing the ID/OOD accuracy, and perhaps understandably, naively combining the two does not maintain their best OOD/ID accuracy. We address this dilemma with the developed **SRAPF**, Stage-wise Retrieval Augmentation-based Adversarial Partial Finetuning. It consists of two finetuning stages: (1) partial finetuning of the visual encoder using both ID and retrieved data, followed by (2) adversarial partial finetuning using few-shot ID data. Extensive experiments on ImageNet-based OOD benchmarks demonstrate that SRAPF significantly outperforms existing VLM adaptation methods in both ID and OOD accuracy.

1 Introduction

Pretrained on diverse web-scale image-text pairs, Vision-Language Models (VLMs) serve as powerful backbones [53, 38] that can achieve strong performance on downstream tasks when adapted with just a few task-specific examples [43]. There exist various adaptation methods, such as prompt tuning [81, 80, 72, 30, 55], adapter learning [13, 78, 59], linear probing [53, 70, 40, 57, 58], and finetuning [43, 16, 33]. Nevertheless, in the real-world applications, the adapted VLM inevitably encounters out-of-distribution (OOD) test data, which deviates from the task-specific in-distribution (ID) training data. The OOD test data challenges the generalization of the adapted VLM. Thus, improving OOD generalization in few-shot adaptation is critically important, motivating our work on *robust few-shot adaptation of VLMs* for both ID and OOD accuracy.

Status Quo. Recent works on few-shot VLM adaptation primarily focus on Parameter-Efficient Finetuning (PEFT), which freezes the VLM and learns a small set of learnable parameters, such

*Corresponding author.

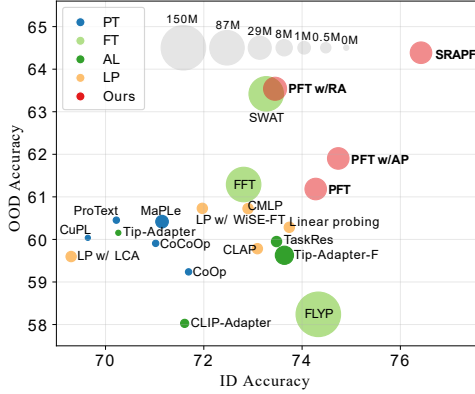


Figure 1: **Comparison of VLM adaptation methods** w.r.t ID and OOD accuracy, as well as numbers of learned parameters. All the methods adapt a pretrained CLIP ViT-B/16 model [53] using 16-shot data sampled from the ImageNet training set. We test them on (1) ImageNet validation set as the ID test-set, and (2) four OOD benchmarks as the OOD test-set (Table 3). We report the mean accuracy across the OOD benchmarks. We roughly categorize these methods into four groups: Prompt Tuning (PT), Finetuning (FT), Adapter Learning (AL), and Linear Probing (LP). Refer to Fig. 3 for more details. Our method **SRAPF** (§ 3.4) significantly outperforms existing adaptation methods in both ID and OOD accuracy.

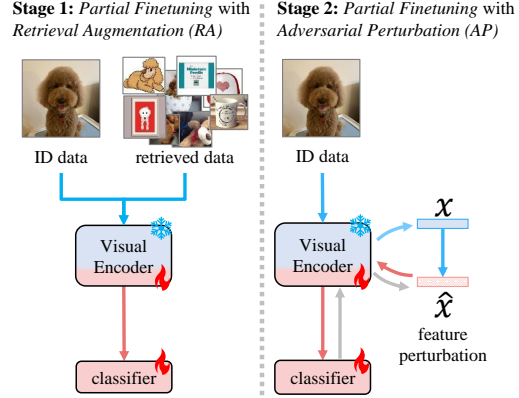


Figure 2: **Flowchart of our few-shot VLM adaptation method SRAPF**, Stage-wise Retrieval Augmentation-based Adversarial Partial Finetuning. In the first stage, SRAPF retrieves task-relevant examples from the VLM’s pretraining dataset to augment the few-shot ID training data and *partially finetunes* the VLM’s visual encoder. In the second stage, SRAPF adversarially perturbs features (Eq. (3)) to augment training data and continues partial finetuning but with only the few-shot ID training data. Results show that *retrieval augmentation* and *adversarial finetuning* greatly improves OOD and ID accuracy (Table 2), and importantly, SRAPF significantly outperforms prior arts w.r.t both ID and OOD accuracy.

as prompt tokens [81, 5, 30, 55, 31], linear classifiers [58, 40, 57], or lightweight adapters [78, 13]. These PEFT methods leverage the VLM’s pretrained features and achieve improved ID and OOD accuracy on downstream tasks. The recent few-shot learning (FSL) work [43] shows that standard finetuning on few-shot training data can yield significantly better ID accuracy than existing PEFT methods, without overfitting concerns. While it does not report OOD accuracy, prior studies show that finetuning can distort pretrained features and degrade OOD generalization [33], and that ensembling the finetuned and the pretrained VLMs can improve both ID and OOD accuracy [70]. Till now, it remains an open question how existing adaptation methods perform w.r.t ID and OOD accuracy when only a few downstream-task or ID training examples are available.

Empirical Findings. Given the inconclusive literature of OOD generalization in few-shot VLM adaptation, we systematically compare existing methods (Fig. 1). Our results show that standard finetuning actually rivals most PEFT methods. We further delve into finetuning methods by comparing contrastive finetuning (CT) [16] and standard finetuning (FT) [53] and analyzing the effect of tuning different network layers. Note that FT finetunes only the visual encoder while CT finetunes both the visual and textual encoder with the contrastive loss used in VLM pretraining [16]. Our analysis reveals two findings (Table 1): (1) finetuning only the top layers achieves superior ID-OOD accuracy balance compared to finetuning entire models; and (2) FT demonstrates both better performance and higher efficiency than CT. Based on these insights, we advocate *partial finetuning* of the visual encoder’s top layers for few-shot VLM adaptation.

Technical Insights. We investigate two simple data augmentation techniques under-explored in the context of OOD generalization: *Retrieval Augmentation (RA)*, and *Adversarial Perturbation (AP)*. While these techniques show promise in other domains, their potential for OOD generalization in few-shot VLM adaptation remains unexplored. First, RA shows significant improvements in zero-shot recognition [50, 42, 66, 25, 36] and few-shot learning [43]. It exploits the VLM’s publicly available pretraining dataset by retrieving task-relevant examples to adapt the VLM. While the retrieved examples inherently exhibit domain gaps with the task-specific data [43], they represent valuable OOD samples that might enhance the OOD generalization of the adapted VLM. Second, AP generates adversarial perturbations to expose model vulnerabilities [45, 14, 4, 62]. Previous works incorporate adversarial perturbations in learning and achieve improved robustness to adversarial attacks [45]. Yet, its potential for robustness to natural distribution shift or OOD generalization remains surprisingly

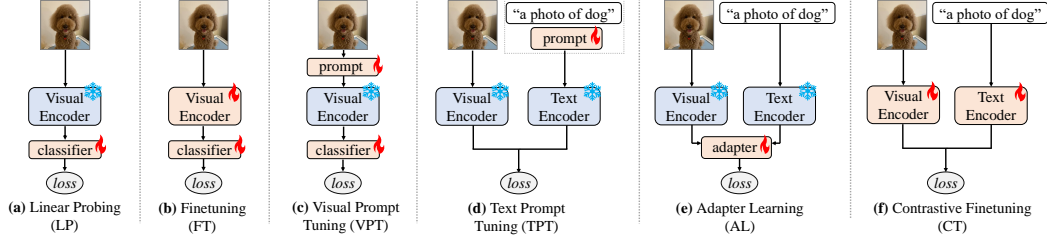


Figure 3: Conceptual frameworks of different adaptation methods. (a) Linear Probing (LP) learns a linear classifier on top of a pretrained visual encoder [53]. (b) Finetuning (FT) learns to update parameters of a pretrained visual encoder over task-specific labeled data [43]. (c) Visual Prompt Tuning (VPT) learns tokens in the input space which are concatenated with image tokens, in addition to the classifier [27]. (d) Text Prompt Tuning (TPT) learns text prompts without updating parameters of the entire VLM [81]. (e) Adapter Learning (AL) extends LP by learning more (layers of) parameters on top of the visual and text encoders [78]. (f) Contrastive Tuning (CT) learns to update parameters of both visual and text encoders using a contrastive loss [16]. We conduct a comprehensive comparison w.r.t both ID and OOD accuracy (Table 3).

unexplored, particularly in few-shot settings. Our experiments reveal that RA and AP independently improve OOD and ID accuracy. However, naively combining them fails to preserve their benefits. We address this dilemma with the proposed SRAPF, a simple and novel stage-wise adaptation pipeline (Fig. 2) that achieves significantly better ID and OOD accuracy (Fig. 1).

Contributions. We make three key contributions:

1. We conduct comprehensive evaluation of representative and recent approaches for few-shot VLM adaptation, such as prompt tuning, linear probing, adapter learning, and finetuning. Our analysis reveals that *partial finetuning* of the visual encoder’s top layers outperforms most of existing methods w.r.t both ID and OOD accuracy (Table 3, Fig. 1).
2. We introduce and evaluate two simple yet effective data augmentation techniques to partial finetuning: *retrieval augmentation-based finetuning*, and *adversarial finetuning*. While these techniques have shown promise in other domains, we demonstrate their first successful application in few-shot VLM adaptation with improved OOD generalization (Table 2).
3. We build on our insights and present **SRAPF**, a simple yet powerful few-shot VLM adaptation pipeline. Extensive experiments on the established ImageNet OOD benchmarks demonstrate that SRAPF significantly outperforms the compared methods in both ID and OOD accuracy (Fig. 1).

2 Related work

Few-Shot VLM Adaptation. VLMs, such as CLIP [53] and ALIGN [26], learn to align images and texts in a shared embedding space through contrastive learning. Trained on diverse web-scale image-text pairs, VLMs [53, 26, 39, 38] exhibit strong zero-shot performance across various visual understanding tasks, such as image captioning [6, 60, 68], visual recognition [53, 50], and visual question answering [18, 60]. To enhance VLM’s performance on specific downstream tasks, numerous studies explore adaptation methods using limited labeled data. Most approaches focus on preserving generalizable features by learning prompt tokens [81, 80, 72, 30, 55] or lightweight adapters [13, 78, 59, 79]. Others investigate full finetuning [43, 16, 33], though [33] shows that this can destroy pretrained features and degrade OOD performance [33]. To mitigate this, [70] proposes ensembling the finetuned and the pretrained models, resulting in improved OOD accuracy at a slight cost to ID performance. However, no prior work has comprehensively compared adaptation methods in terms of OOD generalization. Thus, how to few-shot adapt VLMs with improved ID and OOD performance remains an open question. To address this, we conduct the first comprehensive comparison of existing adaptation methods, deriving key insights that inform our technical contributions.

Robustness and Generalization. In real-world scenarios, training and test data often follow different distributions, requiring machine-learned models to be robust to distribution shifts. To evaluation OOD generalization, prior works have introduced dedicated OOD test sets [67, 54, 21, 2] or proposed methods to predict OOD performance based on ID behavior [46, 1, 28, 57]. Several strategies aim to improve robustness during training, such as data augmentation [51, 77, 48, 22], sophisticated finetuning techniques [33, 16], and model ensembling [70, 69]. Some works focus on adversarial robustness [45, 14, 34, 10] but have not linked relevant solutions to OOD generalization. In this

work, we bridge this gap by leveraging adversarial learning to enhance VLM adaptation, achieving improved OOD generalization.

Retrieval-based Augmentation (RA) retrieves publicly-available open data relevant to a downstream task to enhance predictions when using VLMs [41, 65, 37, 50]. This approach has shown success in multiple domains. In language models, RA improves performance on complex reasoning tasks [20, 35], while in computer vision, it boosts zero-shot recognition [65, 37, 41, 50], few-shot recognition [43], and image generation [7, 3]. Notably, retrieved examples naturally exhibit OOD characteristics compared to task-specific data [42]. This property makes RA particularly valuable for improving OOD generalization. We hypothesize that incorporating RA in few-shot VLM adaptation could enhance the adapted model’s OOD generalization capability. To the best of our knowledge, no prior work has explicitly explored RA for improving OOD generalization in VLM adaptation. Our work addresses this research gap.

Adversarial Learning [14] enhances model robustness by training against crafted adversarial perturbations that aim to mislead the model to wrong predictions. Existing approaches propose generating adversarial examples during training [45, 14, 4, 62], constraining the loss function [74, 15, 12], or regularizing model weights [71, 9]. The seminal work of [45] formulates adversarial training as a min-max optimization problem, using Projected Gradient Descent (PGD) to iteratively generate adversarial examples during training. While this paradigm improves robustness against adversarial attacks [45] and domain generalization [63, 64], its potential for enhancing OOD generalization in *few-shot VLM adaptation* remains unexplored. Our key contribution bridges this gap. We demonstrate that adversarial finetuning of VLMs simultaneously improves both ID and OOD accuracy of the adapted model.

3 Robust Few-Shot Vision-Language Model Adaptation

We begin by formalizing the problem for robust few-shot VLM adaptation. Next, we review representative adaptation methods (Fig. 3) as preliminary background. Lastly, we introduce the proposed techniques and present our final approach SRAPF (Fig. 2).

3.1 Problem Formulation

Training protocol. A pre-trained VLM consists of a text encoder $g(\cdot)$ and a visual encoder $f(\cdot)$. To adapt the VLM for a downstream K -way classification task, we are provided with a small labeled dataset $\mathcal{D} = \{(\mathbf{I}_i, y_i)\}_{i=1}^n$, where \mathbf{I}_i is the i^{th} training image and $y_i \in \{1, \dots, K\}$ is its label. Following the few-shot learning literature [43, 58], we adopt the “ m -shot” setting, where each class has m training examples (thus $n = m * K$). For recognition, the VLM requires textual prompts; each label y_i can be mapped to a textual description as prompt T_i . For instance, for y_i representing the class dog, the corresponding textual prompt T_i can be “a photo of dog”. We denote the image and text embedding features as $\mathbf{x}_i = f(\mathbf{I}_i)$ and $\mathbf{t}_i = g(T_i)$, respectively. In practice, open-source VLMs are pretrained on publicly available datasets, which allow methods to leverage this data to improve the generalization of the adapted models [43].

Evaluation protocol. We evaluate adaptation methods using an ID and OOD test sets. The ID test images follow the same distribution of the task-specific training data (i.e., both are sampled from the same benchmark dataset). All the ID and OOD test sets share the same label space. Note that OOD test data is not accessible during VLM adaptation, therefore, following [33, 16], we rely on the ID validation set for tuning hyperparameters and selecting the checkpoint, which produces the highest top-1 accuracy on this validation set. We run the selected checkpoint on more OOD test sets and report its top-1 accuracies.

3.2 Review of VLM Adaptation Approaches

There are numerous VLM adaptation approaches that make it impossible to enumerate all of them. We categorize these approaches into four major categories (Fig. 3): prompt tuning (PT) including textual PT (TPT) and visual PT (VPT), linear probing (LP), adapter learning (AL), finetuning (FT), and contrastive tuning (CT). Below, we briefly introduce them with high-level descriptions but compare more specific methods of each category in experiments (Table 3).



Figure 4: **Visual comparison** between examples of two ImageNet (IN) classes (as the ID), its OOD variant datasets (marked by blue border), and retrieved VLM’s pretraining data from LAION-400M (marked by orange border). While it is intuitive to think of the retrieved examples as OOD compared to the ID data, they also contain noisy images due to linguistic ambiguity, e.g., lemon also means a pale yellow color hence lemon umbrella is retrieved (the last visual in the first row). Visually, their distributions are different from each other.

Linear Probing (LP), on top of a frozen visual encoder (Fig. 3a), learns a classifier parameterized by $\mathbf{W} = [\mathbf{w}_1, \dots, \mathbf{w}_K]$, where \mathbf{w}_k represents class- k ’s weight parameter. For loss computation, it typically uses the cross entropy (CE): $\ell_{CE}(\mathbf{x}, y) = -\log \frac{\exp(\mathbf{w}_y^T \mathbf{x})}{\sum_{j=1}^K \exp(\mathbf{w}_j^T \mathbf{x})}$. The loss \mathcal{L}_{CE} over a training batch \mathcal{B} , indexing training examples, is computed as:

$$\mathcal{L}_{CE} = \frac{1}{|\mathcal{B}|} \sum_{i \in \mathcal{B}} \ell_{CE}(\mathbf{x}_i, y_i) \quad (1)$$

With a pretrained VLM, it is better to initialize the classifier using embedding features corresponding to the class names [50] than random initialization. Other than learning a classifier, **Full Finetuning (FT)** also updates the visual encoder $f(\cdot)$, commonly also using the CE loss (Fig. 3b).

Contrastive Tuning (CT) finetunes both the visual and text encoders with the contrastive loss \mathcal{L}_{CL} used for pretraining the VLM [16]. It maximizes the cosine similarity between features of matched image-text paired data and minimizes those of unmatched pairs. The loss \mathcal{L}_{CL} is computed as below over a training batch \mathcal{B} :

$$\mathcal{L}_{CL} = -\frac{1}{|\mathcal{B}|} \sum_{i \in \mathcal{B}} \left(\log \frac{\exp(\mathbf{x}_i^T \mathbf{t}_i / \tau)}{\sum_{j \in \mathcal{B}} \exp(\mathbf{x}_i^T \mathbf{t}_j / \tau)} + \log \frac{\exp(\mathbf{x}_j^T \mathbf{t}_i / \tau)}{\sum_{j \in \mathcal{B}} \exp(\mathbf{x}_j^T \mathbf{t}_i / \tau)} \right), \quad (2)$$

where τ is the hyperparameter temperature. Recent work [16] demonstrates that contrastive finetuning a VLM performs better than FT w.r.t ID and OOD accuracy.

Prompt Tuning (PT), a particular PEFT strategy, learns not only a classifier but also some prompt tokens, which are concatenated with the original input into the VLM being frozen during learning. PT can learn textual prompt tokens [81, 80], visual prompt tokens [27], or both [30, 55]. When learning only visual tokens, PT can simply use the CE loss; when the learned prompts contain textual tokens, it usually uses the contrastive loss. In contrast, **Adapter Learning (AL)** usually designs a non-learned module on top of the frozen visual and textual encoders [78, 59]. It may also learn a lightweight module the contrastive loss [13].

3.3 Robust Adaptation for OOD Generalization

Partial finetuning. As reported in [33], full finetuning can distort pretrained features and degrade OOD generalization; yet learning a single classifier over the frozen VLM might learn too few parameters to sufficiently adapt to the given downstream task. We hypothesize that there is a middle ground that finetuning some certain parameters of the VLM achieves better ID and OOD accuracy. We empirically validate this hypothesis by investigating the effects of finetuning different layers (i.e., blocks in ViT network) of the VLM, using both the standard finetuning (FT) and contrastive finetuning (CT). It is important to note that setting a larger learning rate for the classifier remarkably improves FT’s performance (details in Supplement Section E), as reported in [33, 16]. Unsurprisingly, finetuning the top few blocks of parameters yields much better ID and OOD accuracy for both FT and CT, as shown in Table 1. Furthermore, results show that CT does not have a clear advantage over FT w.r.t ID or OOD accuracy when both are configured with well tuned hyperparameters. Hence, for few-shot VLM adaptation, we advocate *partial finetuning (PFT)* of the visual encoder only.

Retrieval Augmentation (RA) is an established technique that leverages publicly available data, such as the VLM’s pretraining dataset LAION-400M [56], to enhance performances on downstream

Table 1: **Partial Contrastive Tuning (PCT)** and **Partial Finetuning (PFT)** of the VLM’s top few blocks yield better ID and OOD accuracy than full finetuning (i.e., “all blocks”) and finetuning the top linear layer (ref. linear probing). Moreover, when selectively finetuning the VLM’s layers, PCT does not show a clear advantage over PFT. Notably, PFT finetunes only the visual encoder, while PCT requires more computes to finetune both the visual and textual encoders. In our experiments, we adopt PFT on the top-4 blocks as the default setting.

finetuned blocks	PCT		PFT		PFT w/ Retrieval Augmentation (RA)					
	ID	OOD	ID	OOD	ID	OOD				
	IN	avg.	IN	avg.	IN	avg.	IN-V2	IN-S	IN-A	IN-R
zero-shot	66.75	57.15	66.75	57.15	66.75	57.15	60.91	46.16	47.53	73.99
top linear layer	72.12	59.50	73.88	60.01	71.11	60.92	64.32	51.06	49.77	78.53
top-1	73.25	60.61	74.93	60.98	72.10	62.27	65.86	51.95	51.33	79.93
top-2	73.62	61.29	75.06	61.28	72.86	62.77	66.53	52.65	51.50	80.41
top-3	73.66	61.47	74.86	61.34	73.23	63.16	66.76	53.42	51.68	80.78
top-4	73.61	61.33	74.29	61.21	73.46	63.54	67.05	53.96	51.16	80.99
top-5	74.48	59.90	73.78	61.03	73.45	63.46	66.61	54.25	51.91	81.09
top-7	74.41	59.31	73.23	61.44	73.34	63.33	66.09	54.34	51.91	80.99
top-9	74.50	59.13	72.99	61.41	73.26	63.24	66.40	54.25	51.58	80.72
top-12 (all blocks)	74.33	58.24	72.81	61.29	73.05	63.29	66.48	54.25	51.71	80.73

tasks [41, 65, 50, 43]. It retrieves task-relevant examples and uses them to adapt pretrained models. [43] reports that the retrieved data has domain gaps compared to task-specific training data (Fig. 4); yet, this might be a good thing in terms of enhancing the adapted model’s OOD generalization capability. Indeed, our experiments validate this point (Table 2). To find task-relevant data, early methods rely on feature similarities between target class names and pretraining images/texts [42, 66]. But this requires downloading, hosting and computing over hundreds of millions of VLM’s pretraining examples. In contrast, recent works use string matching to find relevant text first and retrieve corresponding images [50, 43], showing significantly enhanced efficiency and a capability to retrieve more visually diverse images. As our work is not intended to propose new RA methods, we adopt this string matching-based RA approach [50, 43]. Denote the set of retrieved data, \mathcal{D}_R indexing such data, we compute the CE loss over it: $\mathcal{L}_{RA} = \frac{1}{|\mathcal{D}_R|} \sum_{i \in \mathcal{D}_R} \ell_{CE}(\mathbf{x}_i, y_i)$.

Adversarial Perturbation (AP) perturbs input data by purposefully attacking the learned model. One method of AP is to use projected gradient descent (PGD) to iteratively perturb an input example using the negative loss function (e.g., the CE loss ℓ_{CE}) [14]. Denote this process as $\text{AP}(\mathbf{x}, y; T, \epsilon)$, which returns the perturbed example after iteratively perturbing the input data (\mathbf{x}, y) for T times with magnitude ϵ , i.e., $\hat{\mathbf{x}} = \text{AP}(\mathbf{x}, y; T, \epsilon)$. The t^{th} iteration perturbs data like below (with $\mathbf{x}^0 = \mathbf{x}$): $\mathbf{x}^t = \mathbf{x}^{t-1} + \alpha \cdot \text{sign}(\nabla_{\mathbf{x}} \ell_{CE}(\mathbf{x}^{t-1}, y))$, where α corresponds to the perturbation intensity and ϵ constrains the perturbation range in $[-\epsilon, \epsilon]$ to ensure the adversarial features remain within a bounded neighborhood of the original data. Incorporating AP in learning is shown to improve the robustness of the learned model to adversarial attacks [45]. To contrast the typical CE loss in Eq. (1), we use a separate loss notation to indicate the use of AP:

$$\mathcal{L}_{AP} = \frac{1}{|\mathcal{B}|} \sum_{i \in \mathcal{B}} \ell_{CE}(\text{AP}(\mathbf{x}_i, y_i; T, \epsilon), y_i) \quad (3)$$

Yet, notably, AP has been under-explored in OOD generalization research especially under the few-shot VLM adaptation setting. We apply it on features with PFT (Fig. 2-right) for robust few-shot VLM adaptation, yielding remarkable improvements (Table 2).

3.4 SRAPF: Stage-wise Retrieval Augmentation-based Adversarial Partial Finetuning

Naive combination. With the proposed techniques, RA and AP, to improve the OOD generalization of few-shot VLM adaptation, one may straightforwardly combine them as the final loss²:

$$\mathcal{L} = \mathcal{L}_{CE} + \lambda_{AP} \cdot \mathcal{L}_{AP} + \lambda_{RA} \cdot \mathcal{L}_{RA} \quad (4)$$

where we set $\lambda_{AP} = \lambda_{RA} = 1$ to balance the loss terms. However, our experiments reveal that this does not necessarily improve both ID and OOD accuracy (Table 2). We conjecture the reasons are (1) too much noise in the retrieved examples to make them OOD related to the task-specific data (Fig. 4), and (2) the inherent imbalance in the retrieved data [50, 43]. To address these issues, we propose a stage-wise adaptation pipeline SRAPF.

²When jointly adopting RA and AP, we perform AP on both the task-specific and retrieved data.

Table 2: **Stage-wise finetuning strategies.** The left table compares the results of incorporating RA and AP with PFT and FFT (for reference), along with wall-clock time for 10 epochs of finetuning. The results show that either RA or AP can improve ID or OOD accuracy, with RA yielding significant OOD accuracy gains. Due to the substantial computational overhead of applying them jointly, we propose a two-stage approach with the first stage performing PFT with RA. The right table lists the results of different second-stage finetuning strategies. Applying AP in this stage significantly boosts ID performance while further improving OOD accuracy. We also report the total wall-clock time for 10 epochs of finetuning in this stage, showing that applying AP is quite efficient. Our final approach **SRAPF** (highlighted in blue) combines these insights.

Stage-1		accuracy		wall-clock time (h)
tuning	RA AP	ID	OOD	
FFT	✓	72.81	61.29	0.5
		73.10 ^{+0.29}	63.24 ^{+2.29}	6.4
	✓	73.09 ^{+0.28}	60.58 ^{-0.37}	2.2
	✓ ✓	73.11 ^{+0.30}	63.01 ^{+2.06}	59.2
PFT		74.29	61.21	0.4
	✓	73.46 ^{-0.83}	63.54 ^{+2.33}	3.5
	✓	74.87 ^{+0.58}	61.83 ^{+0.62}	1.0
	✓ ✓	73.55 ^{-0.74}	63.74 ^{+2.53}	20.1

Stage-1		Stage-2		accuracy		wall-clock time (h)
tuning	RA AP	ID	OOD	ID	OOD	
PFT w/ RA				73.45	63.54	3.5
		FFT		75.53 ^{+2.08}	63.71 ^{+0.17}	3.5 + 0.5
		PFT		75.82 ^{+2.37}	64.16 ^{+0.62}	3.5 + 0.4
		PFT	✓	76.44 ^{+2.99}	64.38 ^{+0.84}	3.5 + 1.0
PFT w/ RA+AP				73.55	63.74	20.1
		FFT		75.66 ^{+2.11}	63.92 ^{+0.18}	20.1 + 0.5
		PFT		76.07 ^{+2.52}	64.46 ^{+0.72}	20.1 + 0.4
		PFT	✓	76.50 ^{+2.95}	64.53 ^{+0.79}	20.1 + 1.0

Stage-wise finetuning is shown to mitigate issues caused by imbalanced data distribution [29] and domain gaps [43]. We empirically evaluate different stage-wise strategies (Table 2), and derive the final solution SRAPF, a rather simple yet effective strategy (Fig. 2): (1) using the retrieved and the task-specific data to partially finetune the VLM’s encoder, and (2) incorporating adversarial perturbation of partial finetuning on the visual encoder using the task-specific data only.

4 Experiments

We conduct experiments to investigate finetuning strategies, show PFT is a rather strong method for robust few-shot VLM adaptation, validate the proposed techniques, and demonstrate our final approach SRAPF outperforms existing VLM adaptation methods. We introduce datasets, models, compared methods, and implementation details, before comprehensive experiments.

Datasets and Model. We use ImageNet (IN) [11] as the ID dataset, and its variants as the OOD test sets, including ImageNet-V2 (IN-V2) [54], ImageNet-Sketch (IN-S) [67], ImageNet-Adversarial (IN-A) [24], and ImageNet-Rendition (IN-R) [23]. The four OOD datasets capture different distribution shifts from the original ImageNet, including variations in data collection and labeling, sketches, adversarial images, and artistic renditions. The IN is released for non-commercial research and educational purposes, and the OOD datasets are open-source under the MIT License. Refer to Fig. 4 for their visual examples, and Section B of the Supp for more details of datasets. Following the literature [40, 58, 61, 81, 80], we use the CLIP ViT-B/16 model [53] as the pretrained VLM in experiments. The pretraining dataset of this model is not released to the public, so we use LAION-400M [56] for retrieval augmentation. LAION-400M is open-source under CC-BY 4.0 License and has weak affinity to ImageNet dataset and is more suitable for retrieval-based tasks [8]. We conduct experiments under 4-, 8-, and 16-shot settings, and ablation study in the 16-shot setting.

Compared Methods. We compare representative VLM adaptation methods categorized into prompt tuning [27, 52, 81, 80, 30, 31], adapter learning [78, 13, 73, 79], linear probing [53, 70, 40, 57, 58], and finetuning [70, 16, 43]. Fig. 3 depicts the conceptual difference between these methods. For fair comparison, we run the open-source code of these methods to train on the same ID training data. We include our code as part of the supplementary material. In Section G of the supplementary, we compare them in more detail.

Implementation Details. We implement all the methods with PyTorch and train on a single NVIDIA RTX 4090 GPU (24GB), except CoOp and MaPLe which we run on A40 GPU (48GB). For data augmentation during VLM adaptation, we apply random resize, crop, and horizontal flip. For methods that involve learning, we use the AdamW optimizer and a cosine-annealing learning rate scheduler. We set the learning rates 1e-6 for the backbone and 1e-3 for the classifier, and batch size as 64. We finetune the VLM using our methods for 50 epochs to ensure convergence (though the best-performing checkpoints on the ID validation set are selected around epoch-10). When adopt CT, we set the temperature as 0.01. For AP, we set the max iteration $T = 10$ and magnitude $\epsilon = 0.01$; we analyze the impacts of ϵ in Fig. 5. When using more loss terms (e.g., Eq. (4)), we set their weights as 1.

Table 3: **Benchmarking results of different VLM adaptation methods** on ImageNet (IN) as the ID test set and the OOD variants including ImageNet-V2 (IN-V2), ImageNet-Sketch (IN-S), ImageNet-A (IN-A), and ImageNet-Rendation (IN-R). We categorize existing adaptation methods into four groups: prompt tuning, adapter learning, linear probing, and finetuning. Refer to Fig. 3 for the conceptual illustration of these methods. We run all the methods using the released CLIP ViT-B/16 model [53], under 16-, 8- and 4-shot settings. We report the top-1 accuracy on the IN and OOD benchmarks. For convenient comparison, we report the mean accuracy (marked in **blue**) across the four OOD benchmarks for each method. We list salient conclusions. First, configured with proper hyperparameters, FFT and CT (i.e., FLYP) outperform popular (PEFT) methods. Second, derived from in-depth analysis, PFT rivals FFT and CT. Third, applying either RA or AP to PFT notably improves OOD or ID accuracy. Lastly, our final approach SRAPF significantly outperforms all the compared methods on both ID and OOD accuracy, under all the few-shot settings.

		16-shot						8-shot		4-shot	
		ID		OOD				ID	OOD	ID	OOD
		IN	avg.	IN-V2	IN-S	IN-A	IN-R	IN	avg.	IN	avg.
	method										
Zero-Shot	Prompting [53] <small>ICML'21</small>	66.75	57.15	60.91	46.16	47.53	73.99	66.75	57.15	66.75	57.15
Prompt Tuning	CuPL [52] <small>ICCV'23</small>	69.64	60.04	63.37	49.03	50.68	77.07	69.64	60.04	69.64	60.04
	CoOp [81] <small>IJCV'22</small>	71.69	59.24	64.34	47.20	50.20	75.21	70.80	59.68	70.29	59.74
	CoCoOp* [80] <small>CVPR'22</small>	71.02	59.91	64.07	48.75	50.63	76.18	—	—	—	—
	MaPLe [30] <small>CVPR'23</small>	71.15	60.42	64.49	48.69	50.91	77.58	70.76	60.23	70.58	60.13
	VPT _{shallow} [27] <small>ECCV'22</small>	72.75	60.80	65.70	49.33	49.68	78.56	71.48	60.29	70.31	59.76
	VPT _{deep} [27] <small>ECCV'22</small>	72.78	59.12	65.04	47.83	47.11	76.49	71.22	59.30	70.54	59.71
	ProText* [31] <small>AAAI'25</small>	70.22	60.45	63.54	49.45	51.47	77.35	—	—	—	—
Adapter Learning	Tip-Adapter [78] <small>ECCV'22</small>	70.26	60.16	63.08	48.58	51.09	77.87	69.00	59.87	68.86	59.79
	Tip-Adapter-F [78] <small>ECCV'22</small>	73.64	59.63	65.44	47.88	48.53	76.66	71.78	59.92	70.61	59.96
	CLIP-Adapter [13] <small>IJCV'23</small>	71.61	58.03	64.05	46.66	47.87	73.53	70.25	57.74	69.55	58.36
	TaskRes [73] <small>CVPR'23</small>	73.48	59.95	65.10	48.12	49.96	76.62	71.91	60.04	71.28	59.51
	DMN-ZS* [79] <small>CVPR'24</small>	72.25	63.80	65.17	53.20	58.28	78.55	—	—	—	—
Linear Probing	LP [53] <small>ICML'21</small>	73.74	60.29	65.09	49.07	49.12	77.86	72.45	59.77	71.44	59.55
	LP w/ WiSE-FT [70] <small>CVPR'22</small>	71.97	60.73	64.47	49.43	50.69	78.33	71.37	60.48	70.82	60.20
	CMLP* [40] <small>CVPR'23</small>	72.90	60.73	65.40	49.20	50.50	77.80	—	—	—	—
	LP w/ LCA [57] <small>ICML'24</small>	69.30	59.60	62.41	48.52	49.65	77.81	69.23	59.48	69.15	59.61
	CLAP [58] <small>CVPR'24</small>	73.09	59.78	64.77	47.99	49.73	76.64	71.74	59.74	71.01	59.17
Finetuning	FFT [53] <small>ICML'21</small>	72.81	61.29	65.62	49.27	51.89	78.40	71.74	61.05	70.93	60.70
	FLYP [16] <small>CVPR'23</small>	74.33	58.24	65.50	47.28	45.75	74.43	72.52	58.78	71.80	59.17
	SWAT [43] <small>CVPR'25</small>	73.27	63.42	66.48	54.84	51.30	81.06	72.57	63.01	72.14	62.86
Ours	PFT	74.29	61.21	66.66	49.66	50.99	77.54	72.87	60.62	71.64	60.98
	PFT w/ RA	73.46	63.54	67.05	53.96	51.16	80.99	72.59	63.23	72.06	62.98
	PFT w/ AP	74.87	61.83	67.24	50.29	50.49	79.31	73.51	61.36	72.32	61.26
	SRAPF	76.44	64.38	69.20	54.78	52.19	81.33	75.35	64.28	74.56	63.84

*These results are copied from the original papers.

4.1 Experiment Results

Partial Finetuning (PFT) improves both ID and OOD performance. We first explore the effect of tuning different blocks of the visual encoder using both CT and FT. Note that CT also finetunes the textual encoder: when finetuning the top-X blocks of the visual encoder, it also updates the top-X blocks of the textual encoder. As shown in Table 1, for both FT and CT, finetuning only the top few blocks yields better ID and OOD accuracy than finetuning the top linear layer (ref. linear probing) and all the blocks (i.e., full finetuning). Moreover, when carefully selecting blocks to finetune, CT does not exhibit a clear advantage over FT, challenging the findings of [33, 16], which compares CT and FT under full finetuning. Hereafter, we adopt PFT (finetuning the top-4 blocks) as the default.

Retrieval Augmentation (RA) and Adversarial Perturbation (AP) improve ID and OOD accuracy. Table 2 lists detailed results. Refer to its caption for more conclusions. Jointly applying them does not necessarily preserve their independent ID and OOD accuracy gains, presumably because RA includes too many outlier data (Fig. 4) that hurts adaptation. Moreover, this also requires much more computational overhead. Therefore, we propose stage-wise finetuning, leading to more remarkable improvements. Among different stage-wise finetuning strategies, considering both accuracy and efficiency, we advocate (1) PFT with RA in the first stage, followed by (2) PFT with AP in the second stage. This is our final solution named **SRAPF**.

SRAPF performs the best. Table 3 compares our SRAPF against a multitude of VLM adaptation methods, showing that SRAPF significantly outperforms them w.r.t both ID and OOD accuracy, under all the few-shot settings and on all the OOD benchmarks.

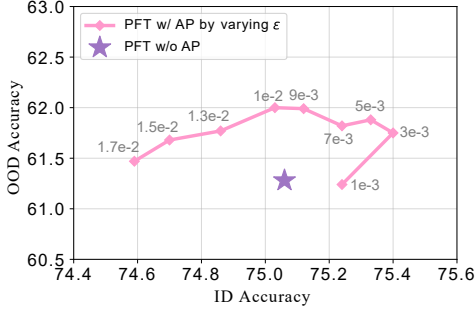


Figure 5: **ID and OOD accuracy w.r.t perturbation magnitude ϵ** by Partial Finetuning (PFT) top-2 blocks with AP (Eq. (3)). We mark the performance of PFT without AP for comparison. With AP, PFT yields improved accuracy on both ID and OOD data. Yet, tuning ϵ leads a trade-off between ID and OOD accuracy. Nevertheless, tuning ϵ based on ID accuracy can still result into a model checkpoint that performs decently on OOD data.

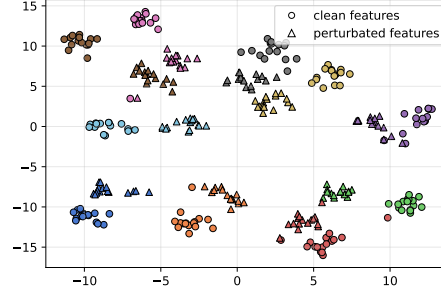


Figure 6: **t-SNE visualization of clean and adversarially perturbed (AP) features** for training images from ten ImageNet classes implies that AP shifts features toward the origin. This aligns with intuition, as directions toward the origin are more likely to adversarially confuse the softmax classifiers. Yet, it also suggests that sophisticated AP methods, capable of generating more diverse perturbations, could further improve the OOD generalization of adapted models.

Impact of perturbation magnitude ϵ . Fig. 5 shows trade-off performance on ID and OOD data by tuning ϵ in AP (Eq. (3)). Importantly, relying on the ID accuracy can help select a checkpoint that yields decent OOD accuracy.

Visualization of perturbed features. Fig. 6 visualizes clean and perturbed features, showing that AP shifts features toward the origin. This makes intuitive sense as directions toward the origin make it easy to confuse softmax classifiers. This analysis also suggests that future AP methods that can produce diverse perturbations could help improve OOD generalization further.

5 Discussions on Broad Impacts and Limitations

Broad Impacts. Few-shot VLM adaptation has broad applications, such as assisting data annotation where a task’s annotation guidelines provide a few visual examples exploitable for adaptation [44]. Enhancing the OOD generalization of adapted VLMs is practically significant in numerous applications like clinical diagnosis [47] and autonomous driving [49, 44], where the adapted models must reliably generalize to OOD test data. Our work advances robust few-shot VLM adaptation, enriching the research landscape. However, we note that improved OOD generalization may lead over-generalization, where the model can fail to alert when encountering open-set [32], anomalous [17], counterfactual [76], or adversarial [75] test data. This could lead to negative societal impacts.

Limitations and Future Work. Our work has certain limitations that warrant discussion. First, RA may not work well in highly specialized tasks involving customized data that is distinct from publicly available datasets. Second, while the vanilla AP method proves effective, the perturbed examples lack diversity, e.g., primarily shifting examples towards the origin to adversarially confuse classifier (Fig. 6). Diversifying adversarial perturbations could further improve OOD generalization, suggesting future work in controllable adversarial perturbation towards specific classes. Third, although following prior work that relies on an ID validation set for hyperparameter tuning and model selection, we note that a large validation set is often unavailable in real-world applications [40, 58, 43]. Future work could exploit RA to construct an OOD validation set.

6 Conclusions

We study robust few-shot VLM adaptation for downstream tasks with limited labeled examples. Our systematic evaluation of existing adaptation methods demonstrates that *partial finetuning* of the VLM’s top layers yields better ID and OOD accuracy than full finetuning or simply learning a linear classifier. We base on these insights and incorporate two simple yet effective techniques from related domains: *Retrieval Augmentation* and *Adversarial Perturbation* to improve the adapted model’s OOD generalization. By incorporating these techniques, we propose a rather powerful stage-wise finetuning pipeline **SRAPF**. Extensive experiments demonstrate that SRAPF significantly outperforms existing methods w.r.t both ID and OOD accuracy.

References

- [1] Christina Baek, Yiding Jiang, Aditi Raghunathan, and J Zico Kolter. Agreement-on-the-line: Predicting the performance of neural networks under distribution shift. In *Advances in Neural Information Processing Systems (NeurIPS)*, volume 35, pages 19274–19289, 2022.
- [2] Andrei Barbu, David Mayo, Julian Alverio, William Luo, Christopher Wang, Dan Gutfreund, Josh Tenenbaum, and Boris Katz. Objectnet: A large-scale bias-controlled dataset for pushing the limits of object recognition models. In *Advances in Neural Information Processing Systems (NeurIPS)*, volume 32, 2019.
- [3] Andreas Blattmann, Robin Rombach, Kaan Oktay, Jonas Müller, and Björn Ommer. Retrieval-augmented diffusion models. In *Advances in Neural Information Processing Systems (NeurIPS)*, 2022.
- [4] Nicholas Carlini and David Wagner. Towards evaluating the robustness of neural networks. In *2017 IEEE Symposium on Security and Privacy (SP)*, pages 39–57. Ieee, 2017.
- [5] Guangyi Chen, Weiran Yao, Xiangchen Song, Xinyue Li, Yongming Rao, and Kun Zhang. Plot: Prompt learning with optimal transport for vision-language models. In *International Conference on Learning Representations (ICLR)*, 2023.
- [6] Jun Chen, Han Guo, Kai Yi, Boyang Li, and Mohamed Elhoseiny. Visualgpt: Data-efficient adaptation of pretrained language models for image captioning. In *Proceedings of the IEEE/CVF Conference on Computer Vision and Pattern Recognition (CVPR)*, 2022.
- [7] Wenhui Chen, Hexiang Hu, Chitwan Saharia, and William W Cohen. Re-imagen: Retrieval-augmented text-to-image generator. In *International Conference on Learning Representations (ICLR)*, 2023.
- [8] Mehdi Cherti, Romain Beaumont, Ross Wightman, Mitchell Wortsman, Gabriel Ilharco, Cade Gordon, Christoph Schuhmann, Ludwig Schmidt, and Jenia Jitsev. Reproducible scaling laws for contrastive language-image learning. In *Proceedings of the IEEE/CVF Conference on Computer Vision and Pattern Recognition (CVPR)*, pages 2818–2829, 2023.
- [9] Moustapha Cisse, Piotr Bojanowski, Edouard Grave, Yann Dauphin, and Nicolas Usunier. Parseval networks: Improving robustness to adversarial examples. In *International conference on machine learning (ICML)*. PMLR, 2017.
- [10] Francesco Croce and Matthias Hein. Reliable evaluation of adversarial robustness with an ensemble of diverse parameter-free attacks. In *International Conference on Machine Learning (ICML)*, pages 2206–2216. PMLR, 2020.
- [11] Jia Deng, Wei Dong, Richard Socher, Li-Jia Li, Kai Li, and Li Fei-Fei. Imagenet: A large-scale hierarchical image database. In *Proceedings of the IEEE/CVF Conference on Computer Vision and Pattern Recognition (CVPR)*, 2009.
- [12] Pierre Foret, Ariel Kleiner, Hossein Mobahi, and Behnam Neyshabur. Sharpness-aware minimization for efficiently improving generalization. In *International conference on machine learning (ICML)*, 2021.
- [13] Peng Gao, Shijie Geng, Renrui Zhang, Teli Ma, Rongyao Fang, Yongfeng Zhang, Hongsheng Li, and Yu Qiao. Clip-adapter: Better vision-language models with feature adapters. *International Journal of Computer Vision (IJCV)*, 132(2):581–595, 2023.
- [14] Ian J Goodfellow, Jonathon Shlens, and Christian Szegedy. Explaining and harnessing adversarial examples. *arXiv preprint arXiv:1412.6572*, 2014.
- [15] Sven Gowal, Jonathan Uesato, Chongli Qin, Po-Sen Huang, Timothy Mann, and Pushmeet Kohli. An alternative surrogate loss for pgd-based adversarial testing. *arXiv preprint arXiv:1910.09338*, 2019.
- [16] Sachin Goyal, Ananya Kumar, Sankalp Garg, Zico Kolter, and Aditi Raghunathan. Finetune like you pretrain: Improved finetuning of zero-shot vision models. In *Proceedings of the IEEE/CVF Conference on Computer Vision and Pattern Recognition (CVPR)*, 2023.
- [17] Zhaopeng Gu, Bingke Zhu, Guibo Zhu, Yingying Chen, Ming Tang, and Jinqiao Wang. Anomalygpt: Detecting industrial anomalies using large vision-language models. In *Proceedings of the AAAI conference on artificial intelligence (AAAI)*, volume 38, pages 1932–1940, 2024.
- [18] Jiaxian Guo, Junnan Li, Dongxu Li, Anthony Meng Huat Tiong, Boyang Li, Dacheng Tao, and Steven Hoi. From images to textual prompts: Zero-shot visual question answering with frozen large language models. In *Proceedings of the IEEE/CVF Conference on Computer Vision and Pattern Recognition (CVPR)*, pages 10867–10877, 2023.

- [19] Yunhui Guo, Honghui Shi, Abhishek Kumar, Kristen Grauman, Tajana Rosing, and Rogerio Feris. Spottune: transfer learning through adaptive fine-tuning. In *Proceedings of the IEEE/CVF Conference on Computer Vision and Pattern Recognition (CVPR)*, pages 4805–4814, 2019.
- [20] Kelvin Guu, Kenton Lee, Zora Tung, Panupong Pasupat, and Mingwei Chang. Retrieval augmented language model pre-training. In *International Conference on Machine Learning (ICML)*, volume 119, pages 3929–3938, 2020.
- [21] Dan Hendrycks and Thomas Dietterich. Benchmarking neural network robustness to common corruptions and perturbations. In *International Conference on Learning Representations (ICLR)*, 2019.
- [22] Dan Hendrycks, Norman Mu, Ekin D Cubuk, Barret Zoph, Justin Gilmer, and Balaji Lakshminarayanan. Augmix: A simple data processing method to improve robustness and uncertainty. In *International conference on machine learning (ICLR)*, 2020.
- [23] Dan Hendrycks, Steven Basart, Norman Mu, Saurav Kadavath, Frank Wang, Evan Dorundo, Rahul Desai, Tyler Zhu, Samyak Parajuli, Mike Guo, et al. The many faces of robustness: A critical analysis of out-of-distribution generalization. In *Proceedings of the IEEE/CVF International Conference on Computer Vision (ICCV)*, 2021.
- [24] Dan Hendrycks, Kevin Zhao, Steven Basart, Jacob Steinhardt, and Dawn Song. Natural adversarial examples. In *Proceedings of the IEEE/CVF Conference on Computer Vision and Pattern Recognition (CVPR)*, pages 15262–15271, 2021.
- [25] Ahmet Iscen, Mathilde Caron, Alireza Fathi, and Cordelia Schmid. Retrieval-enhanced contrastive vision-text models. In *International Conference on Learning Representations (ICLR)*, 2024.
- [26] Chao Jia, Yinfei Yang, Ye Xia, Yi-Ting Chen, Zarana Parekh, Hieu Pham, Quoc Le, Yun-Hsuan Sung, Zhen Li, and Tom Duerig. Scaling up visual and vision-language representation learning with noisy text supervision. In *International Conference on Machine Learning (ICML)*, pages 4904–4916. PMLR, 2021.
- [27] Menglin Jia, Luming Tang, Bor-Chun Chen, Claire Cardie, Serge Belongie, Bharath Hariharan, and Ser-Nam Lim. Visual prompt tuning. In *European Conference on Computer Vision (ECCV)*, pages 709–727. Springer, 2022.
- [28] Yiding Jiang, Vaishnavh Nagarajan, Christina Baek, and J Zico Kolter. Assessing generalization of SGD via disagreement. In *International Conference on Learning Representations (ICLR)*, 2022.
- [29] Bingyi Kang, Saining Xie, Marcus Rohrbach, Zhicheng Yan, Albert Gordo, Jiashi Feng, and Yannis Kalantidis. Decoupling representation and classifier for long-tailed recognition. *arXiv preprint arXiv:1910.09217*, 2019.
- [30] Muhammad Uzair Khattak, Hanoona Rasheed, Muhammad Maaz, Salman Khan, and Fahad Shahbaz Khan. Maple: Multi-modal prompt learning. In *Proceedings of the IEEE/CVF Conference on Computer Vision and Pattern Recognition (CVPR)*, pages 19113–19122, 2023.
- [31] Muhammad Uzair khattak, Muhammad Ferjad, Naseer Muzzamal, Luc Van Gool, and Federico Tombari. Learning to prompt with text only supervision for vision-language models. In *Proceedings of the AAAI Conference on Artificial Intelligence (AAAI)*, 2025.
- [32] Shu Kong and Deva Ramanan. Opendan: Open-set recognition via open data generation. In *Proceedings of the IEEE/CVF International Conference on Computer Vision (ICCV)*, October 2021.
- [33] Ananya Kumar, Aditi Raghunathan, Robbie Matthew Jones, Tengyu Ma, and Percy Liang. Fine-tuning can distort pretrained features and underperform out-of-distribution. In *International Conference on Learning Representations (ICLR)*, 2022.
- [34] Alexey Kurakin, Ian J Goodfellow, and Samy Bengio. Adversarial examples in the physical world. In *Artificial intelligence safety and security*, pages 99–112. Chapman and Hall/CRC, 2018.
- [35] Patrick Lewis, Ethan Perez, Aleksandra Piktus, Fabio Petroni, Vladimir Karpukhin, Naman Goyal, Heinrich Küttler, Mike Lewis, Wen-tau Yih, Tim Rocktäschel, Sebastian Riedel, and Douwe Kiela. Retrieval-augmented generation for knowledge-intensive nlp tasks. In *Advances in Neural Information Processing Systems (NeurIPS)*, volume 33, pages 9459–9474, 2020.
- [36] Alexander Li, Ellis Brown, Alexei A Efros, and Deepak Pathak. Internet explorer: Targeted representation learning on the open web. In *International Conference on Machine Learning (ICML)*, 2023.

- [37] Alexander Cong Li, Ellis Langham Brown, Alexei A Efros, and Deepak Pathak. Internet explorer: Targeted representation learning on the open web. In *International Conference on Machine Learning (ICML)*, volume 202, pages 19385–19406, 2023.
- [38] Junnan Li, Ramprasaath Selvaraju, Akhilesh Gotmare, Shafiq Joty, Caiming Xiong, and Steven Chu Hoi. Align before fuse: Vision and language representation learning with momentum distillation. In *Advances in Neural Information Processing Systems (NeurIPS)*, volume 34, pages 9694–9705, 2021.
- [39] Junnan Li, Dongxu Li, Caiming Xiong, and Steven Hoi. Blip: Bootstrapping language-image pre-training for unified vision-language understanding and generation. In *International Conference on Machine Learning (ICML)*, pages 12888–12900. PMLR, 2022.
- [40] Zhiqiu Lin, Samuel Yu, Zhiyi Kuang, Deepak Pathak, and Deva Ramanan. Multimodality helps unimodality: Cross-modal few-shot learning with multimodal models. In *Proceedings of the IEEE/CVF Conference on Computer Vision and Pattern Recognition (CVPR)*, pages 19325–19337, 2023.
- [41] Haotian Liu, Kilho Son, Jianwei Yang, Ce Liu, Jianfeng Gao, Yong Jae Lee, and Chunyuan Li. Learning customized visual models with retrieval-augmented knowledge. In *Proceedings of the IEEE/CVF Conference on Computer Vision and Pattern Recognition (CVPR)*, pages 15148–15158, June 2023.
- [42] Haotian Liu, Kilho Son, Jianwei Yang, Ce Liu, Jianfeng Gao, Yong Jae Lee, and Chunyuan Li. Learning customized visual models with retrieval-augmented knowledge. In *Proceedings of the IEEE/CVF Conference on Computer Vision and Pattern Recognition (CVPR)*, 2023.
- [43] Tian Liu, Huixin Zhang, Shubham Parashar, and Shu Kong. Few-shot recognition via stage-wise retrieval-augmented finetuning. In *Proceedings of the IEEE/CVF Conference on Computer Vision and Pattern Recognition (CVPR)*, 2025.
- [44] Anish Madan, Neehar Peri, Shu Kong, and Deva Ramanan. Revisiting few-shot object detection with vision-language models. In *Advances in Neural Information Processing Systems (NeurIPS)*, 2024.
- [45] Aleksander Madry, Aleksandar Makelov, Ludwig Schmidt, Dimitris Tsipras, and Adrian Vladu. Towards deep learning models resistant to adversarial attacks. *arXiv preprint arXiv:1706.06083*, 2017.
- [46] John P Miller, Rohan Taori, Aditi Raghunathan, Shiori Sagawa, Pang Wei Koh, Vaishaal Shankar, Percy Liang, Yair Carmon, and Ludwig Schmidt. Accuracy on the line: on the strong correlation between out-of-distribution and in-distribution generalization. In *International Conference on Machine Learning (ICML)*, pages 7721–7735. PMLR, 2021.
- [47] Jong Hak Moon, Hyungyung Lee, Woncheol Shin, Young-Hak Kim, and Edward Choi. Multi-modal understanding and generation for medical images and text via vision-language pre-training. *IEEE Journal of Biomedical and Health Informatics*, 26(12):6070–6080, 2022.
- [48] Junsoo Oh and Chulhee Yun. Provable benefit of cutout and cutmix for feature learning. In *Advances in Neural Information Processing Systems (NeurIPS)*, 2024.
- [49] Chenbin Pan, Burhaneddin Yaman, Tommaso Nesti, Abhirup Mallik, Alessandro G Allievi, Senem Velipasalar, and Liu Ren. Vlp: Vision language planning for autonomous driving. In *Proceedings of the IEEE/CVF Conference on Computer Vision and Pattern Recognition (CVPR)*, pages 14760–14769, 2024.
- [50] Shubham Parashar, Zhiqiu Lin, Tian Liu, Xiangjue Dong, Yanan Li, Deva Ramanan, James Caverlee, and Shu Kong. The neglected tails in vision-language models. In *Proceedings of the IEEE/CVF Conference on Computer Vision and Pattern Recognition (CVPR)*, 2024.
- [51] Francesco Pinto, Harry Yang, Ser Nam Lim, Philip Torr, and Puneet Dokania. Using mixup as a regularizer can surprisingly improve accuracy & out-of-distribution robustness. *Advances in Neural Information Processing Systems (NeurIPS)*, 35:14608–14622, 2022.
- [52] Sarah Pratt, Ian Covert, Rosanne Liu, and Ali Farhadi. What does a platypus look like? generating customized prompts for zero-shot image classification. In *Proceedings of the IEEE/CVF International Conference on Computer Vision (ICCV)*, pages 15691–15701, 2023.
- [53] Alec Radford, Jong Wook Kim, Chris Hallacy, Aditya Ramesh, Gabriel Goh, Sandhini Agarwal, Girish Sastry, Amanda Askell, Pamela Mishkin, Jack Clark, et al. Learning transferable visual models from natural language supervision. In *International Conference on Machine Learning (ICML)*, pages 8748–8763. PMLR, 2021.

- [54] Benjamin Recht, Rebecca Roelofs, Ludwig Schmidt, and Vaishaal Shankar. Do imagenet classifiers generalize to imagenet? In *International Conference on Machine Learning (ICML)*, pages 5389–5400. PMLR, 2019.
- [55] Shuvendu Roy and Ali Etemad. Consistency-guided prompt learning for vision-language models. In *International Conference on Learning Representations (ICLR)*, 2024.
- [56] Christoph Schuhmann, Richard Vencu, Romain Beaumont, Robert Kaczmarczyk, Clayton Mullis, Aarush Katta, Theo Coombes, Jenia Jitsev, and Aran Komatsuzaki. Laion-400m: Open dataset of clip-filtered 400 million image-text pairs. *arXiv preprint arXiv:2111.02114*, 2021.
- [57] Jia Shi, Gautam Gare, Jinjin Tian, Siqi Chai, Zhiqiu Lin, Arun Vasudevan, Di Feng, Francesco Ferroni, and Shu Kong. LCA-on-the-line: benchmarking out-of-distribution generalization with class taxonomies. In *Proceedings of the 41st International Conference on Machine Learning (ICML)*, 2024.
- [58] Julio Silva-Rodriguez, Sina Hajimiri, Ismail Ben Ayed, and Jose Dolz. A closer look at the few-shot adaptation of large vision-language models. In *Proceedings of the IEEE/CVF Conference on Computer Vision and Pattern Recognition (CVPR)*, 2024.
- [59] Lin Song, Ruoyi Xue, Hang Wang, Hongbin Sun, Yixiao Ge, Ying Shan, et al. Meta-adapter: An online few-shot learner for vision-language model. In *Advances in Neural Information Processing Systems (NeurIPS)*, volume 36, pages 55361–55374, 2023.
- [60] Zeyi Sun, Ye Fang, Tong Wu, Pan Zhang, Yuhang Zang, Shu Kong, Yuanjun Xiong, Dahua Lin, and Jiaqi Wang. Alpha-clip: A clip model focusing on wherever you want. In *Proceedings of the IEEE/CVF Conference on Computer Vision and Pattern Recognition (CVPR)*, pages 13019–13029, 2024.
- [61] Junjiao Tian, Zecheng He, Xiaoliang Dai, Chih-Yao Ma, Yen-Cheng Liu, and Zsolt Kira. Trainable projected gradient method for robust fine-tuning. In *Proceedings of the IEEE/CVF Conference on Computer Vision and Pattern Recognition (CVPR)*, pages 7836–7845, 2023.
- [62] Florian Tramèr, Alexey Kurakin, Nicolas Papernot, Ian Goodfellow, Dan Boneh, and Patrick McDaniel. Ensemble adversarial training: Attacks and defenses. In *International Conference on Learning Representations (ICLR)*, 2018.
- [63] Riccardo Volpi, Pietro Morerio, Silvio Savarese, and Vittorio Murino. Adversarial feature augmentation for unsupervised domain adaptation. In *Proceedings of the IEEE Conference on Computer Vision and Pattern Recognition (CVPR)*, pages 5495–5504, 2018.
- [64] Riccardo Volpi, Hongseok Namkoong, Ozan Sener, John C Duchi, Vittorio Murino, and Silvio Savarese. Generalizing to unseen domains via adversarial data augmentation. *Advances in Neural Information Processing Systems (NeurIPS)*, 31, 2018.
- [65] Matthew Wallingford, Vivek Ramanujan, Alex Fang, Aditya Kusupati, Roozbeh Mottaghi, Aniruddha Kembhavi, Ludwig Schmidt, and Ali Farhadi. Neural priming for sample-efficient adaptation. In *Advances in Neural Information Processing Systems (NeurIPS)*, volume 36, pages 65566–65584, 2023.
- [66] Matthew Wallingford, Vivek Ramanujan, Alex Fang, Aditya Kusupati, Roozbeh Mottaghi, Aniruddha Kembhavi, Ludwig Schmidt, and Ali Farhadi. Neural priming for sample-efficient adaptation. In *Advances in Neural Information Processing Systems (NeurIPS)*, 2023.
- [67] Haohan Wang, Songwei Ge, Zachary Lipton, and Eric P Xing. Learning robust global representations by penalizing local predictive power. In *Advances in Neural Information Processing Systems (NeurIPS)*, 2019.
- [68] Weihang Wang, Qingsong Lv, Wenmeng Yu, Wenyi Hong, Ji Qi, Yan Wang, Junhui Ji, Zhuoyi Yang, Lei Zhao, Song XiXuan, et al. Cogvlm: Visual expert for pretrained language models. In *Advances in Neural Information Processing Systems (NeurIPS)*, 2025.
- [69] Mitchell Wortsman, Gabriel Ilharco, Samir Ya Gadre, Rebecca Roelofs, Raphael Gontijo-Lopes, Ari S Morcos, Hongseok Namkoong, Ali Farhadi, Yair Carmon, Simon Kornblith, et al. Model soups: averaging weights of multiple fine-tuned models improves accuracy without increasing inference time. In *International Conference on Machine Learning (ICML)*. PMLR, 2022.
- [70] Mitchell Wortsman, Gabriel Ilharco, Jong Wook Kim, Mike Li, Simon Kornblith, Rebecca Roelofs, Raphael Gontijo Lopes, Hannaneh Hajishirzi, Ali Farhadi, Hongseok Namkoong, et al. Robust fine-tuning of zero-shot models. In *Proceedings of the IEEE/CVF Conference on Computer Vision and Pattern Recognition (CVPR)*, pages 7959–7971, 2022.

- [71] Dongxian Wu, Shu-Tao Xia, and Yisen Wang. Adversarial weight perturbation helps robust generalization. In *Advances in Neural Information Processing Systems (NeurIPS)*, 2020.
- [72] Hantao Yao, Rui Zhang, and Changsheng Xu. Visual-language prompt tuning with knowledge-guided context optimization. In *Proceedings of the IEEE/CVF Conference on Computer Vision and Pattern Recognition (CVPR)*, pages 6757–6767, 2023.
- [73] Tao Yu, Zhihe Lu, Xin Jin, Zhibo Chen, and Xinchao Wang. Task residual for tuning vision-language models. In *Proceedings of the IEEE/CVF Conference on Computer Vision and Pattern Recognition (CVPR)*, 2023.
- [74] Hongyang Zhang, Yaodong Yu, Jiantao Jiao, Eric Xing, Laurent El Ghaoui, and Michael Jordan. Theoretically principled trade-off between robustness and accuracy. In *International Conference on Machine Learning (ICML)*. PMLR, 2019.
- [75] Jiaming Zhang, Qi Yi, and Jitao Sang. Towards adversarial attack on vision-language pre-training models. In *Proceedings of the 30th ACM International Conference on Multimedia (ACMMM)*, pages 5005–5013, 2022.
- [76] Letian Zhang, Xiaotong Zhai, Zhongkai Zhao, Yongshuo Zong, Xin Wen, and Bingchen Zhao. What if the tv was off? examining counterfactual reasoning abilities of multi-modal language models. In *Proceedings of the IEEE/CVF Conference on Computer Vision and Pattern Recognition (CVPR)*, pages 21853–21862, 2024.
- [77] Linjun Zhang, Zhun Deng, Kenji Kawaguchi, Amirata Ghorbani, and James Zou. How does mixup help with robustness and generalization? In *International Conference on Learning Representations (ICLR)*, 2021.
- [78] Renrui Zhang, Wei Zhang, Rongyao Fang, Peng Gao, Kunchang Li, Jifeng Dai, Yu Qiao, and Hongsheng Li. Tip-adapter: Training-free adaption of clip for few-shot classification. In *European Conference on Computer Vision (ECCV)*, pages 493–510. Springer, 2022.
- [79] Yabin Zhang, Wenjie Zhu, Hui Tang, Zhiyuan Ma, Kaiyang Zhou, and Lei Zhang. Dual memory networks: A versatile adaptation approach for vision-language models. In *Proceedings of the IEEE/CVF Conference on Computer Vision and Pattern Recognition (CVPR)*, pages 28718–28728, 2024.
- [80] Kaiyang Zhou, Jingkang Yang, Chen Change Loy, and Ziwei Liu. Conditional prompt learning for vision-language models. In *Proceedings of the IEEE/CVF Conference on Computer Vision and Pattern Recognition (CVPR)*, pages 16816–16825, 2022.
- [81] Kaiyang Zhou, Jingkang Yang, Chen Change Loy, and Ziwei Liu. Learning to prompt for vision-language models. *International Journal of Computer Vision (IJCV)*, 130(9):2337–2348, 2022.

Robust Few-Shot Vision-Language Model Adaptation

(Supplemental Document)

This document supports our main paper with detailed results and comprehensive analysis. The document is organized as follows:

- **Section A.** We provide code to reproduce our proposed methods.
- **Section B.** We provide a detailed summary of datasets used in our experiments and show more examples of training and testing data.
- **Section C.** We provide the details of open data retrieval.
- **Section D.** We provide hyperparameters used in our work.
- **Section E.** We provide the results of PFT using the same learning rate for the backbone and classifier.
- **Section F.** We provide full results on PCT and PFT.
- **Section G.** We provide more details of the compared methods.
- **Section H.** We provide an analysis of the loss weight λ_{AP} in PFT w/ AP.
- **Section I.** We provide more discussions on limitations and future work.

A Code

We include our code as part of the supplementary material, comprising the following key components:

Requirements. Running the code requires Python, PyTorch, and other common packages. We list all dependencies in the *requirements.txt* file for convenient installation. Additionally, we include detailed environment setup instructions in the *README.md* file. Below are the versions of Python and PyTorch used in this work:

- Python: 3.10.16
- PyTorch: 1.12.0

License. We will release our code under the MIT license.

Instructions. We provide detailed instructions for reproducing our experiments in the following markdown files:

- *DATASETS.md* provides detailed steps for installing the datasets used in our experiments, including ImageNet OOD benchmarks, few-shot splits and retrieval dataset.
- *README.md* provides detailed guidelines on how to set up the environment and run the demo of the proposed methods.

Demo. The code includes three demos to demonstrate the results of our proposed methods in Table 3. In the demonstration, we finetune CLIP ViT-B/16 model for 16-shot learning using ImageNet (IN) as the ID dataset and evaluate the methods both on ImageNet and its four variants, including ImageNet-V2 (IN-V2) [54], ImageNet-Sketch (IN-S) [67], ImageNet-Adversarial (IN-A) [24], and ImageNet-Rendition (IN-R) [23]. The details of the demos are as follows:

- *PFT_demo.ipynb* contains the implementation of **Partial Finetuning**. We finetune the top-4 blocks by default.
- *PFT_w_AP_demo.ipynb* contains the implementation of **Partial Finetuning with Adversarial Perturbation** with a perturbation magnitude ϵ of 0.01.
- *SRAPF_demo.ipynb* contains the implementation of **Stage-wise Retrieval Augmentation-based Adversarial Partial Finetuning**.



Figure 7: **Comparison of ImageNet training data (as ID), its four variants (as OOD, marked by blue border), and retrieved data from LAION-400M (marked by orange border).** To illustrate the distributional characteristics, we present more examples of the training and testing images by randomly selecting four classes from ImageNet. The visual comparison reveals significant distribution shifts between ID and OOD data. In addition, although the retrieved data enhances sample diversity, it also introduces noisy images due to linguistic ambiguity in the retrieval process.

B Summary of Datasets

We summarize the datasets used in our experiments in Table 4. Following established protocols from prior work [33, 40, 58], we report the ID accuracy using ImageNet validation set [11], and OOD performance on the ImageNet variants [54, 67, 24, 23]. For few-shot adaptation, we sample training data from the official ImageNet training set. All methods are evaluated using three independent training runs with different random seeds for data splitting. Fig. 7 presents additional comparative examples from ImageNet and its four variants, illustrating the distribution differences across these datasets.

Table 4: **Statistics of datasets for evaluating OOD generalization.** We list the number of images in the official training, validation, and test sets for ImageNet and its variants. The protocol of OOD generalization samples few-shot data from the official training set; we use them as *our train set* to adapt the VLM, and evaluate its performance on ImageNet variants.

dataset	# cls	train	val	test	dataset description
IN [11]	1,000	1.28M	50,000	N/A	sampling images for 1,000 common classes
IN-V2 [54]	1,000	N/A	N/A	10,000	sampling OOD images of the ImageNet’s 1,000 classes
IN-S [67]	1,000	N/A	N/A	50,000	sampling sketches for ImageNet’s 1,000 classes
IN-A [24]	200	N/A	N/A	7,500	sampling adversarial images for 200 ImageNet’s classes
IN-R [23]	200	N/A	N/A	30,000	sampling artistic, cartoon, and sketch renditions for 200 ImageNet’s classes

C Details of Data Retrieval

Following previous works [41, 43], we retrieve images from LAION-400M [56] based on the string matching. As illustrated in Fig. 8, the retrieved data distribution for ImageNet exhibits a typical long-tail pattern. This distribution imbalance persists across different pretrained datasets such as LAION-400M and MetaCLIP [50]. For each class, we implement a selection protocol whereby samples are ranked by text-to-text similarity and the top-500 most relevant images are retained, yielding a final dataset of 471,876 images. We display more examples of the retrieved data in Fig. 7.

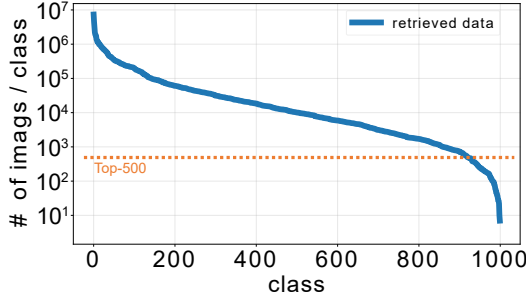


Figure 8: **The retrieved data of ImageNet from LAION-400M follows an imbalanced distribution.** For our data retrieval process, we employ string matching to identify relevant samples, subsequently selecting the 500 most similar images (based on text-to-text feature similarity) per class for inclusion in the training set.

D Hyperparameters

For our experiments, we use a validation set to tune hyperparameters. We follow the practice in [43, 40, 50, 70] to initialize classifier with the average text embedding of OpenAI 80 prompts. For adversarial perturbation, we maintain a 1:1 ratio between clean and adversarial features, i.e., we generate one adversarial counterpart for each clean feature. A comprehensive list of all hyperparameters used in our experiments is provided in Table 5.

Table 5: **We list the hyperparameters for our methods**, including PFT, PFT w/ RA, PFT w/ AP, and SRAPF.

Methods	PFT	PFT w/ RA	PFT w/ AP	SRAPF: stage-1	SRAPF: stage-2
epochs	50	10	50	10	10
batch size	64	64	64	64	64
optimizer			AdamW		
lr for backbone			1e-6		
lr for classifier			1e-3		
lr schedule			CosineAnnealingLP		
weight decay	0.1	0.01	0.1	0.01	0.01
warmup iters			18		
warmup lr			1e-8		
data augmentation		RandomResizedCrop, RandomHorizontalFlip			
λ_{RA}	–	1.0	–	1.0	–
λ_{AP}	–	–	1.0	–	1.0
ϵ	–	–	0.01	–	0.01

E Tuning Learning Rates for Partial Finetuning

We study how learning rates affect the final performance by comparing “varied learning rates” and “uniform learning rate”. In the varied learning rate setting, we follow prior work [33] to set a larger rate for the classifier. Specifically, we employ 1e-6 for the CLIP backbone while utilizing a larger rate of 1e-3 for the classifier. Conversely, the uniform learning rate condition applies 1e-6 to both the backbone and classifier. We report the ID and average OOD accuracy in Table 6. These results demonstrate that appropriate hyperparameter selection can substantially enhance ID performance while maintaining comparable OOD performance.

F Full Results of Partial Tuning

Table 7 presents complete results across four OOD datasets, comparing two partial tuning approaches: Partial Contrastive Tuning (PCT), which employs contrastive loss, and Partial Finetuning (PFT), which utilizes cross entropy loss. It should be noted that when finetuning the top-X blocks under contrastive loss (i.e., PCT), we finetune both the visual and text encoders’ top-X blocks using the same learning rate. The results demonstrate that both PCT and PFT consistently outperform full finetuning (i.e., top-12 blocks), achieving superior performance on both ID and OOD accuracy. Moreover, PFT is more computationally efficient compared with PCT, while maintaining competitive performance.

Table 6: **Applying varied learning rates (LR) outperforms** uniform learning rate for partial finetuning, especially on ID accuracy.

finetuned blocks	w/ varied LR		w/ uniform LR	
	ID	OOD	ID	OOD
	IN	avg.	IN	avg.
zero-shot	66.75	57.15	66.75	57.15
top linear layer	73.88	60.01	72.29	59.78
top-1	74.93	60.98	72.92	60.80
top-2	75.06	61.28	72.99	61.52
top-3	74.86	61.34	73.03	61.68
top-4	74.29	61.21	72.86	61.50
top-5	73.78	61.03	72.67	61.36
top-7	73.23	61.44	72.23	61.05
top-9	72.99	61.41	72.00	61.21
top-12 (all blocks)	72.81	61.29	71.88	61.26

Table 7: **Full OOD benchmark results of Partial Contrastive Tuning (PCT) and Partial Finetuning (PFT)** for CLIP ViT-B/16 model under 16-shot settings. The experimental results demonstrate that partial tuning surpasses full finetuning w.r.t ID and OOD performance. In addition, PFT shows no advantage over PCT in terms of either computational efficiency or model effectiveness. Results are comparable to Table 1.

finetuned blocks	Partial Contrastive Tuning (PCT)						Partial Finetuning (PFT)					
	ID		OOD				ID		OOD			
	IN	avg.	IN-V2	IN-S	IN-A	IN-R	IN	avg.	IN-V2	IN-S	IN-A	IN-R
zero-shot	66.75	57.15	60.91	46.16	47.53	73.99	66.75	57.15	60.91	46.16	47.53	73.99
top linear layer	72.12	59.50	63.97	48.19	49.20	76.64	73.88	60.01	65.62	48.69	48.21	77.51
top-1	73.25	60.61	65.48	48.78	50.71	77.48	<u>74.93</u>	60.98	66.95	49.42	49.40	78.15
top-2	73.62	61.29	66.19	49.41	51.68	77.89	75.06	61.28	67.09	<u>49.73</u>	50.43	77.88
top-3	73.66	61.47	<u>66.27</u>	49.41	52.07	78.14	74.86	61.34	<u>66.99</u>	49.79	51.00	77.57
top-4	73.61	61.33	66.30	49.21	51.79	78.02	74.29	61.21	66.66	49.66	50.99	77.54
top-5	74.48	59.90	66.04	48.60	49.57	75.37	73.78	61.03	66.37	49.32	51.12	77.33
top-7	<u>74.41</u>	59.31	66.11	47.73	48.81	74.58	73.23	61.44	66.26	49.68	51.36	78.45
top-9	74.50	59.13	66.02	47.86	48.03	74.61	72.99	<u>61.41</u>	65.98	49.50	<u>51.80</u>	78.35
top-12 (all blocks)	74.33	58.24	65.50	47.28	45.75	74.43	72.81	61.29	65.62	49.27	51.89	<u>78.40</u>

G Details of Compared Methods

We roughly divide our compared methods into the following four categories:

- **Prompt Tuning** methods adapt VLM through learnable prompt tokens without adapting the whole VLM. Among them, CoOp [81] and CoCoOp [80] optimize text prompt tokens for the language branch, while VPT [27] introduces learnable prompts for visual inputs. MaPLe [30] simultaneously learns prompts for both visual and textual modalities. ProText [31] leverages large language model knowledge to learn text prompts without visual supervision.
- **Adapter Learning** methods adapt VLM by learning more parameters on top of the visual and text encoders. Tip-Adapter [78] implements a key-value cache mechanism derived from few-shot training examples. CLIP-Adapter [13] introduces an adapter consisting of two linear layers. TaskRes [73] learns a target task classifier by optimizing a set of task-specific residual parameters. DMN-ZS [79] proposes dual memory networks to preserve knowledge of few-shot training data and testing data.
- **Linear Probing** methods adapt pretrained VLM by training a linear classifier on the frozen visual encoder. LP w/ WiSE-FT [70] employs weight-space ensembling, combining classifier weights with the pretrained model (We use an interpolation factor of 0.5 in our experiment). CMLP [40] leverages multimodal examples as additional training examples. LP w/ LCA [57] introduces WordNet class hierarchy as the soft label. CLAP [58] introduces class-adaptive penalty terms during classifier training.
- **Finetuning** methods adapt VLM by updating all parameters for downstream tasks. Standard finetuning method only finetunes the visual encoder with cross entropy loss, while FLYP [16]

Table 8: **Averaged accuracy with standard deviations.** For each method, we run three times using different few-shot training data and report the average accuracy and standard deviation on ImageNet (as ID dataset) and its variants (as OOD datasets). Our proposed methods demonstrate superior accuracy and stability.

methods		ID		OOD				
		IN	IN-V2	IN-S	IN-A	IN-R	avg.	
Prompt Tuning	CoOp [81] <small>ICV'22</small>	71.74±0.16	64.57±0.22	47.54±0.31	50.40±0.25	75.58±0.36	59.52±0.28	
	MaPLe [30] <small>CVPR'23</small>	71.05±0.17	64.27±0.33	48.74±0.45	50.72±0.20	77.22±0.34	60.24±0.29	
	VPT _{shallow} [27] <small>ECCV'22</small>	72.61±0.20	65.51±0.30	49.08±0.21	49.72±0.47	78.51±0.13	60.70±0.23	
	VPT _{deep} [27] <small>ECCV'22</small>	72.63±0.14	65.14±0.23	47.67±0.23	47.28±0.50	76.59±0.16	59.17±0.26	
Adapter Learning	Tip-Adapter [78] <small>ECCV'22</small>	70.22±0.06	63.18±0.10	48.64±0.07	51.07±0.21	77.81±0.06	60.17±0.06	
	Tip-Adapter-F [78] <small>ECCV'22</small>	73.39±0.27	65.38±0.05	47.94±0.24	48.99±0.49	76.96±0.26	59.81±0.16	
	CLIP-Adapter [13] <small>ICV'23</small>	71.48±0.14	63.88±0.15	46.49±0.20	47.65±0.58	73.78±0.36	57.95±0.25	
	TaskRes [73] <small>CVPR'23</small>	73.42±0.10	65.27±0.19	48.08±0.05	49.27±0.70	76.93±0.29	59.89±0.16	
Linear Probing	LP [53] <small>ICML'21</small>	73.67±0.13	65.40±0.33	48.83±0.30	49.37±0.26	77.57±0.32	60.29±0.09	
	LP w/ WiSE-FT [70] <small>CVPR'22</small>	71.93±0.04	64.66±0.22	49.44±0.01	50.62±0.07	78.33±0.03	60.76±0.04	
	LP w/ LCA [57] <small>ICML'24</small>	69.34±0.07	62.53±0.11	48.52±0.02	49.47±0.19	77.76±0.05	59.57±0.05	
	CLAP [58] <small>CVPR'24</small>	73.04±0.08	64.94±0.15	47.91±0.07	49.59±0.27	76.97±0.28	59.85±0.09	
Finetuning	FFT [53] <small>ICML'21</small>	72.71±0.10	65.49±0.13	49.30±0.21	51.86±0.40	78.42±0.05	61.27±0.08	
	FLYP [16] <small>CVPR'23</small>	74.14±0.16	65.50±0.05	47.29±0.09	45.43±0.62	74.82±0.34	58.26±0.13	
	SWAT [43] <small>CVPR'25</small>	73.47±0.17	66.67±0.26	54.84±0.06	51.12±0.09	81.26±0.18	63.49±0.06	
Ours	PFT	74.29±0.09	66.45±0.20	49.69±0.19	50.84±0.24	77.55±0.12	61.13±0.09	
	PFT w/RA	73.43±0.02	66.99±0.06	54.01±0.06	51.66±0.44	80.99±0.01	63.50±0.04	
	PFT w/AP	74.69±0.16	67.04±0.20	50.16±0.31	50.32±0.84	79.15±0.14	61.67±0.18	
	SRAPF	76.50±0.07	69.32±0.19	54.81±0.09	52.05±0.13	81.23±0.11	64.35±0.03	

finetunes both visual and textual encoders using contrastive loss. SWAT [43] proposes a two-stage method with retrieval augmentation for few-shot learning.

To evaluate the performance stability of both baseline and proposed methods, we conduct three runs with different few-shot training data splits and compute the mean accuracy and standard deviations. Results in Table 8 demonstrate that our methods exhibit low variance and hence better stability.

H The Impacts of the λ_{AP} Coefficient

We analyze the impact of the λ_{AP} coefficient in Eq. 4 on the performance of PFT (top-2 blocks) with AP. As shown in Table 9, finetuning top-2 blocks of the visual encoder with only adversarial samples (ref. “no clean samples”) improves OOD accuracy by 0.1% but reduces ID performance. By incorporating clean samples during training, PFT with AP can enhance OOD generalization while maintaining ID accuracy. Specifically, employing an equal weight between these two sample types (i.e., $\lambda_{AP} = 1$) yields an OOD accuracy improvement of 0.72% with negligible impact on ID performance.

λ_{AP} value	ID		OOD			
	IN	avg.	IN-V2	IN-S	IN-A	IN-R
0	75.06	61.28	67.09	49.73	50.43	77.88
0.25	75.27	62.06	67.21	50.35	51.31	<u>79.36</u>
1.00	75.03	<u>62.00</u>	67.40	<u>50.30</u>	<u>50.92</u>	79.39
1.50	74.97	61.81	67.33	50.15	50.55	79.22
4.00	74.81	61.76	<u>67.35</u>	50.17	50.44	79.09
no clean samples	74.79	61.40	67.00	49.95	49.87	78.80

Table 9: **Ablation study on the loss weight λ_{AP}** by partial finetuning top-2 blocks with AP. The results indicate that joint training on both clean and adversarial samples can improve OOD performance without compromising ID accuracy. We set λ_{AP} to 1 as the default.

I More Discussions

Our work does not dig into whether Contrastive Tuning (CT) might benefit from different number of tuning blocks in the visual and textual encoders. Future work exploring asymmetric tuning could be insightful. It would be interesting to develop methods to automatically determine what layers to finetune similar in spirit to pre-VLM works [19].

Although we follow the literature that uses the CLIP ViT-B/16 model and ImageNet-based OOD benchmarks [40, 58, 61, 81, 80], future work should study adaptation methods on more foundation models with different network architectures and benchmark datasets. It would be interesting to study how adaptation methods are robust to different levels of class imbalance in a given downstream task.